Half-Integer Quantized Topological Response in Quasiperiodically Driven Quantum Systems

P. J. D. Crowley,[1,*] I. Martin,[2] and A. Chandran[1]
[1]Department of Physics, Boston University, Boston, Massachusetts 02215, USA
[2]Materials Science Division, Argonne National Laboratory, Argonne, Illinois 60439, USA

(Received 19 September 2019; revised 19 December 2019; accepted 4 August 2020; published 31 August 2020)

A spin strongly driven by two harmonic incommensurate drives can pump energy from one drive to the other at a quantized average rate, in close analogy with the quantum Hall effect. The pumping rate is a nonzero integer in the topological regime, while the trivial regime does not pump. The dynamical transition between the regimes is sharp in the zero-frequency limit and is characterized by a Dirac point in a synthetic band structure. We show that the pumping rate is *half-integer* quantized at the transition and present universal Kibble-Zurek scaling functions for energy transfer processes. Our results adapt ideas from quantum phase transitions, quantum information, and topological band theory to nonequilibrium dynamics, and identify qubit experiments to observe the universal linear and nonlinear response of a Dirac point in synthetic dimensions.

DOI: 10.1103/PhysRevLett.125.100601

Introduction.—A wide variety of classical and quantum systems undergo second-order phase transitions in equilibrium [1–6]. Near such transitions, a universal coarse-grained description emerges; this predicts, for example, the same fluctuations for the fluid density near the liquid-gas critical point as the magnetization near the Ising paramagnet-ferromagnet transition. Far from equilibrium, the description of phase transitions is more complicated. Although a number of dynamical transitions have been observed in driven dissipative systems [7–20], comparatively little is known about their general theory.

Here we consider a dynamical phase transition in probably the simplest possible setting: a spin-$\frac{1}{2}$ driven by two drives with incommensurate frequencies. The drives may be produced by two optical cavities prepared in coherent states [Fig. 1(a)]. The driving increases the richness of the problem by introducing two "synthetic dimensions," which correspond to the photon numbers in the two cavities [21–25]. More precisely, the stationary states of the two-tone driven spin-$\frac{1}{2}$ are given by the stationary states of a two-dimensional synthetic tight-binding model in the presence of an electric field which is equal to the vector of drive frequencies (ω_1, ω_2) [21–30].

For a range of parameters, the tight-binding model in synthetic dimensions exhibits the quantum Hall effect [24,25,30,31]. Reference [24] first identified the corresponding response in the driven qubit system: an average integer quantized energy current between the two drives in a direction set by the polarization of the qubit [Figs. 1(a)–1(c)]. Reference [25] further identified other quantized responses in generic two-tone driven qudits and the integer topological invariant controlling these effects.

In this Letter, we show that the dynamical transition between the topological (pumping) and the trivial (nonpumping) regimes exhibits a half-integer quantized energy pumping rate [Figs. 1(b)–1(c)]. The transition is sharp in

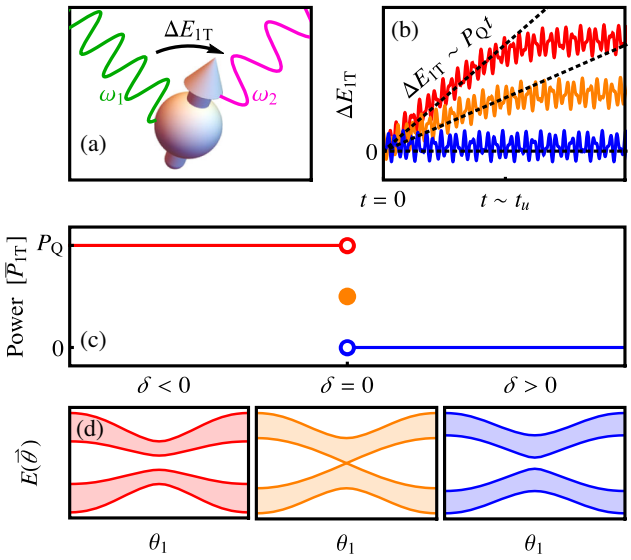

FIG. 1. (a) A spin driven by two incommensurate drives can transfer energy ΔE_{1T} from one drive to the other. (b) The mean rate of energy transfer (power) is topologically quantized up to the unlock time t_u. (c) For $t \ll t_u$, the mean power jumps from $P_Q = (\omega_1\omega_2/2\pi)$ in the topologically nontrivial regime ($\delta < 0$) to zero in the trivial regime ($\delta > 0$). At the transition ($\delta = 0$), the mean power is $P_Q/2$. (d) The instantaneous energies of the Hamiltonian [Eq. (2)] organized into a band structure as a function of θ_1. At the transition, the band structure contains a Dirac point that controls the universal low-frequency response.

the zero-frequency limit. At the transition, the band structure of the synthetic model in the absence of the electric field has a Dirac point [Fig. 1(d)]. The half-integer quantization follows from the integrated Berry curvature of one of the bands excluding the Dirac point.

To observe the quantized energy current the spin's evolution must be nearly adiabatic and "locked" in an instantaneous eigenstate. Away from the zero-frequency limit, the pumping is thus a prethermal effect. Using Kibble-Zurek (KZ) arguments [32–44], we show the time t_u when the spin unlocks to diverge as

$$t_u \sim \sqrt{B_0/\omega^3}, \tag{1}$$

where B_0 is the typical amplitude of the instantaneous field, and $\omega = \sqrt{\omega_1\omega_2}$ is the typical frequency of the drives. On the timescales larger than t_u, the spin's direction is effectively decoupled from the external drives, leading to zero average pumping rate [Fig. 1(b)].

Near the transition, we show that the pump power is universal when measured in units of the diverging timescale t_u. The pump power has two universal contributions: one of topological origins that is quantized to either an integer or a half-integer as $t/t_u \to 0$, and another nonquantized contribution due to spin excitation. Drawing intuition from the action of time reversal on Hall insulators, we isolate the two contributions and their associated universal Kibble-Zurek scaling functions using time evolution with the Hamiltonian and its complex conjugate. Experimentally, complex conjugation corresponds to reversing the circular polarization of one drive. Incommensurately driven few-level quantum systems thus offer a unique window into the universal properties of the topological phase transitions of band insulators.

Model.—For concreteness, we work with the same model as Refs. [24,25,30] in which a spin $\frac{1}{2}$ is driven by two circularly polarized magnetic fields:

$$H(\vec{\theta}_t) = -\frac{1}{2}\vec{B}(\vec{\theta}_t)\cdot\vec{\sigma},$$
$$\vec{B}(\vec{\theta}_t) = B_0(\sin\theta_{t1}, \sin\theta_{t2}, 2+\delta-\cos\theta_{t1}-\cos\theta_{t2}), \tag{2}$$

where $\vec{\theta}_t = (\theta_{t1}, \theta_{t2})$ is the vector of drive phases, $\theta_{ti} = \omega_i t + \theta_{0i}$, and the ratio of the drive frequencies ω_2/ω_1 is an irrational number. We assume that the ratio of drive frequencies is order 1, so that $\omega = \sqrt{\omega_1\omega_2}$ is the single frequency scale on which H varies. The spin operator is a vector of Pauli matrices, $\vec{\sigma} = (\sigma_x, \sigma_y, \sigma_z)$; the spin is initialized in the instantaneous ground state.

Instantaneous band structure.—At each $\vec{\theta}$, the instantaneous eigenstates of $H(\vec{\theta})$ are either aligned or antialigned with the instantaneous magnetic field $\vec{B}(\vec{\theta})$, with eigenvalues $\mp|\vec{B}(\vec{\theta})|/2$, respectively. We organize these instantaneous eigenstates into a band structure on the torus $\vec{\theta} \in [0, 2\pi)^2$. The instantaneous band structure describes the qubit dynamics for $t \ll t_u$ when the spin's evolution remains adiabatic.

The Hamiltonian in Eq. (2) is engineered so that the instantaneous band structure is topologically nontrivial. Specifically, the instantaneous band structure is identical to the momentum-space band structure of a simple model of a quantum Hall insulator, the so-called half-BHZ model [31,45,46]. Consequently, the instantaneous ground state band (corresponding to the eigenvalue $-|\vec{B}(\vec{\theta})|/2$) has a nonzero Chern number $C_g = 1$ for $-2 < \delta < 0$, and $C_g = 0$ for $\delta > 0$.

In the vicinity of the transition at $\delta = 0$, there is a massive Dirac point in the band structure at $|\vec{\theta}| = 0$ [Fig. 1(d)]:

$$H(\vec{\theta}) = -\frac{B_0}{2}(\theta_1\sigma_x + \theta_2\sigma_y + \delta\sigma_z) + O(|\vec{\theta}|^2). \tag{3}$$

Figure 2 is a density plot of the Berry curvature of the ground state band in the topological regime, close to the transition. The Berry curvature has two contributions: a piece that is smooth in δ and $\vec{\theta}$ and integrates to π; and a singular piece that concentrates into a delta function at $\vec{\theta} = \vec{0}$ and integrates to $-\mathrm{sgn}(\delta)\pi$ [31,45].

The drive phases follow trajectories of constant slope in $\vec{\theta}$ space (shown in blue in Fig. 2). Consider $t \ll t_u$. Away from the Dirac point, the Berry curvature is small, and the spin state along the trajectory approximately follows the instantaneous ground state [47]. In the low frequency limit and with ω_2/ω_1 irrational, the trajectory uniformly samples this Berry curvature over time.

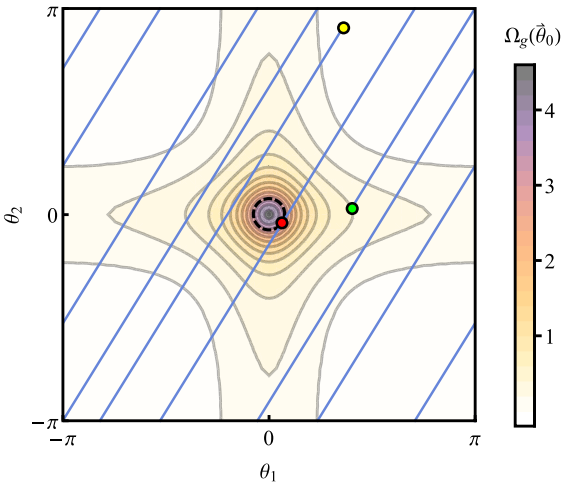

FIG. 2. Contour plot of the Berry curvature of the instantaneous ground state band near the transition ($\delta = -1/3$). Blue lines depict the trajectory of the drive phases. The integrated Berry curvature sets the (average) energy pumping rate until the spin enters the excitation region $|\vec{\theta}_t| < \theta^*$ (dashed circle) for the first time (red point).

We show below [Eq. (9)] that the average power is set by the integrated Berry curvature of the instantaneous ground state band before unlock. Sufficiently far away from the transition, the trajectory thus samples the entire Berry curvature. At the transition, however, the spin unlocks before sampling the singular component associated with the Dirac point. Thus, the integrated Berry curvature that sets the average power is given by

$$C_g = \begin{cases} 1 & \delta < 0 \\ \frac{1}{2} & \delta = 0 \\ 0 & \delta > 0. \end{cases} \tag{4}$$

Pump power.—The instantaneous rate of energy transfer from drive 1 is given by [24]

$$P_1 \equiv \omega_1 \langle \partial_{\theta_1} H \rangle, \tag{5}$$

with a corresponding expression for P_2. As the spin cannot absorb energy indefinitely, the net energy flux into the system time averages to zero, $[P_{\mathrm{tot}}]_t = [P_1]_t + [P_2]_t = 0$. Throughout, $[\cdot]_x$ denotes averaging with respect to variable x.

In the low frequency limit, P_1 is a sum of two terms, one analytic and one nonanalytic in ω. The analytic term is completely determined by the instantaneous values of $\vec{\theta}_t$, while the nonanalytic terms depend on the entire history of the trajectory. As in the Landau-Zener problem, the analytic terms describe the perturbative "dressing" of the spin state over the instantaneous ground state [47–49]. The nonanalytic terms capture the nonadiabatic excitation processes between the dressed states. Below we refer to the leading order analytic term as P_{1T}, as it is of topological origin, and the nonanalytic term as P_{1E}, which is due to excitations.

Topological contribution to pumping for $t \ll t_u$.—Let $|\tilde{g}(\vec{\theta}_t)\rangle$ be the spin state dressed to order ω above the instantaneous ground state. Thus,

$$\begin{aligned} i\frac{d|\tilde{g}\rangle}{dt} &= H|\tilde{g}\rangle + O(\omega^2) \\ &\Rightarrow H|\tilde{g}\rangle = i\omega_1|\partial_{\theta_1}\tilde{g}\rangle + i\omega_2|\partial_{\theta_2}\tilde{g}\rangle + O(\omega^2). \end{aligned} \tag{6}$$

where we have suppressed the time dependence of $\vec{\theta}$ for brevity. Using the product rule and Eq. (6), we obtain

$$\begin{aligned} P_{1T} &= \omega_1 \langle \tilde{g}|\partial_{\theta_1} H|\tilde{g}\rangle \\ &= \omega_1 [\partial_{\theta_1}\langle \tilde{g}|H|\tilde{g}\rangle - \langle \partial_{\theta_1}\tilde{g}|H|\tilde{g}\rangle - \langle \tilde{g}|H|\partial_{\theta_1}\tilde{g}\rangle] \\ &= \omega_1 \partial_{\theta_1}\langle \tilde{g}|H|\tilde{g}\rangle + \omega_1\omega_2\Omega_{\tilde{g}}(\vec{\theta}), \end{aligned} \tag{7}$$

where $\Omega_{\tilde{g}}(\vec{\theta}) = 2\mathrm{Im}\langle \partial_{\theta_1}\tilde{g}|\partial_{\theta_2}\tilde{g}\rangle$ is the Berry curvature of the dressed spin state.

The instantaneous power varies with the initial phase vector $\vec{\theta}_0$. Universal results about the spin dynamics at each t follow upon initial phase averaging

$$[P_{1T}]_{\vec{\theta}_0} = [\partial_{\theta_{1t}}\langle \tilde{g}|H|\tilde{g}\rangle]_{\vec{\theta}_0} + \omega_1\omega_2[\Omega_{\tilde{g}}(\vec{\theta}_t)]_{\vec{\theta}_0}. \tag{8}$$

The first term vanishes as it is a total derivative. The second term is the integrated Berry curvature of the dressed band prior to unlock (and thus excludes the Dirac point). As the integrated Berry curvature of the dressed and instantaneous bands are identical, we obtain

$$[P_{1T}]_{\vec{\theta}_0} = C_g P_{\mathrm{Q}} \equiv C_g \frac{\omega_1\omega_2}{2\pi}, \tag{9}$$

with C_g given by Eq. (4). Formally Eq. (9) holds at fixed δ as $\omega \to 0, t/t_u \to 0$.

Kibble-Zurek estimate for t_u.—The probability to transition to the dressed instantaneous excited state follows from the Landau-Zener result [49–52]

$$p_{\mathrm{exc}} \sim \max_t \exp\left(-\frac{\pi|\vec{B}(\vec{\theta}_t)|^2}{|\partial_t \vec{B}|}\right). \tag{10}$$

Deep in the topological or trivial regimes, the spin's evolution thus remains adiabatic for an exponentially long timescale $\sim \exp(B_0/\omega)$.

Equation (10) predicts that the spin unlocks from the field when the instantaneous gap squared becomes comparable or smaller than the rate of change of the field [32–36,38,41–43]. At the transition, the spin thus unlocks when

$$|\vec{\theta}_t| \lesssim \theta^* := \sqrt{\omega/B_0}. \tag{11}$$

This relation defines the "excitation region" within the dashed circle in Fig. 2(a). A typical spin trajectory enters the excitation region for the first time after $2\pi/\theta^*$ periods. We thus obtain the scaling of the unlock time $t_u \sim (\omega\theta^*)^{-1} \sim \sqrt{B_0/\omega^3}$ previously stated in Eq. (1).

Topological contribution to pumping for $t \gg t_u$.—At times much longer than the unlock time, nonadiabatic processes heat the spin. In the initial phase ensemble, the populations in the (dressed) instantaneous ground and excited states thus become equal. As the Chern numbers of the ground and excited state bands sum to zero, the ensemble averaged power $[P_{1\mathrm{T}}]_{\vec{\theta}_0} \to 0$ as $t/t_u \to \infty$.

Excitation contribution to pumping.—The nonadiabatic excitation of the spin results in a distinct contribution to the power $[P_{1\mathrm{E}}]_{\vec{\theta}_0}$. As the spin absorbs order B_0 energy from the drives over a timescale t_u

$$[P_{1\mathrm{E}}]_{\vec{\theta}_0} \sim B_0/t_u \propto \omega^{3/2}, \qquad t \lesssim t_u. \tag{12}$$

Unlike the topological contribution, the power due to excitation is nonanalytic in ω. The total pumped power is the sum of the topological and excitation contributions.

A constant rate of excitation results in a linear increase of the excited state population in the initial phase ensemble at

small t/t_u. At late times, the populations become equal, and statistically the spin ceases to absorb energy from the drives. Thus, $[P_{1E}]_{\vec{\theta}_0} \to 0$ as $t/t_u \to \infty$.

Kibble-Zurek scaling functions.—Within the Kibble-Zurek (KZ) scaling limit, the nonequilibrium dynamics of the spin becomes universal even beyond the unlock time. The KZ scaling limit involves taking $\omega, \delta \to 0$ together while measuring time in units of the diverging unlock time t_u, and the drive frequency in units of the vanishing scale $\omega^* \sim B_0\delta^2$ [34,37,39–43]. The KZ scaling limit accesses the "critical fan" around the $\omega = 0, \delta = 0$ transition, while Eq. (9) applies deep within each "dynamical phase" (at fixed δ) as $\omega \to 0$.

In the KZ scaling limit, the radius of the excitation region θ^* becomes small and the Hamiltonian of the massive Dirac cone [Eq. (3)] controls the excitation of the spin, and hence the decay of the topological component of the power. The topological and excitation components of the power then take the following scaling forms:

$$[P_{1E}(t;\omega,\delta)]_{\vec{\theta}_0} \sim \omega^{3/2}\mathcal{P}_{1E}(t\omega^{3/2};\delta\omega^{-1/2}),$$
$$[P_{1T}(t;\omega,\delta)]_{\vec{\theta}_0} \sim \frac{\omega^2}{2\pi}\mathcal{P}_{1T}(t\omega^{3/2};\delta\omega^{-1/2}). \quad (13)$$

Above, $\mathcal{P}_{1E}$ and $\mathcal{P}_{1T}$ are scaling functions determined solely by the universality class of the transition in the instantaneous band structure. They capture the universal crossover from the prethermal regime to the late-time infinite-temperature regime.

Scaling functions for the Dirac transition.—We now numerically extract the scaling forms $\mathcal{P}_{1E}, \mathcal{P}_{1T}$ for the Dirac transition in the half-BHZ model by comparing the trajectories generated by $H(\vec{\theta}_t)$ and the complex-conjugated Hamiltonian $H'(\vec{\theta}_t) = [H(\vec{\theta}_t)]^*$. Physically, H' is implemented by flipping the chirality of one of the circularly polarized drives. As this flips the sign of $[P_{1T}]_{\vec{\theta}_0}$ alone, we can separate the topological and excitation contributions to the pumped power:

$$[P_{1E}]_{\vec{\theta}_0} = \frac{1}{2}([P_1]_{\vec{\theta}_0} + [P_1']_{\vec{\theta}_0}),$$
$$[P_{1T}]_{\vec{\theta}_0} = \frac{1}{2}([P_1]_{\vec{\theta}_0} - [P_1']_{\vec{\theta}_0}), \quad (14)$$

Here, $P_1' = \omega_1\langle\psi_t'|\partial_{\theta_1}H'(\vec{\theta}_t)|\psi_t'\rangle$ is the instantaneous rate of energy transfer from drive 1 in the conjugated system $i\partial_t|\psi_t'\rangle = H'(\vec{\theta}_t)|\psi_t'\rangle$ when it is initialized in its instantaneous ground-state band $|\psi_0'\rangle = (|\psi_0\rangle)^*$. In the Supplemental Material [53], we obtain the same scaling functions for a different microscopic model with a Dirac transition, demonstrating universality.

In more detail, Eq. (14) is obtained as follows. As the probability of excitation in Eq. (10) is invariant under complex conjugation, the ensemble populations of the instantaneous eigenstates are the same at each t/t_u for time evolution under H and H'. Thus, $[P_{1E}']_{\vec{\theta}_0} = [P_{1E}]_{\vec{\theta}_0}$. The topological piece, however, changes sign, $[P_{1T}']_{\vec{\theta}_0} = -[P_{1T}]_{\vec{\theta}_0}$ as the Berry curvature changes sign under complex conjugation.

Figure 3 shows the scaling functions across the transition for both contributions for small t/t_u. The excitation scaling function is proportional to excitation probability for $t \ll t_u$. As $p_{exc} \sim \exp(-\delta^2 B_0/\omega)$, Fig. 3(a) is thus well fit by a Gaussian centered at the transition (black-white dashed line).

Figure 3(b) shows $[P_{1T}]/P_Q$ to obey a single-parameter scaling function at fixed t/t_u, with the $[P_{1T}]/P_Q \to 1(0)$ as $\delta \to -\infty(\infty)$ [Eq. (4)]. The intermediate value at $\delta = 0$ is close to $\frac{1}{2}$, and becomes exactly $\frac{1}{2}$ as $t/t_u \to 0$. For $\delta\omega^{-1/2} = \mathrm{O}(1)$, the component of the Berry curvature that is singular at the transition has a width comparable to that of the excitation region θ^*. Consequently, this component is partially sampled by spin trajectories before unlock and leads to the smooth universal function observed in Fig. 3(b). Note that Eq. (9) is contained within the scaling function in Eq. (13) on taking $\omega \to 0$ at fixed δ.

A technical comment: the data in Fig. 3 is time averaged over $t\omega^{3/2} \in [0, 1.72]$ (in addition $\vec{\theta}_0$ averaging). This reduces fluctuations due to the finite sampling of $\vec{\theta}_0$ and

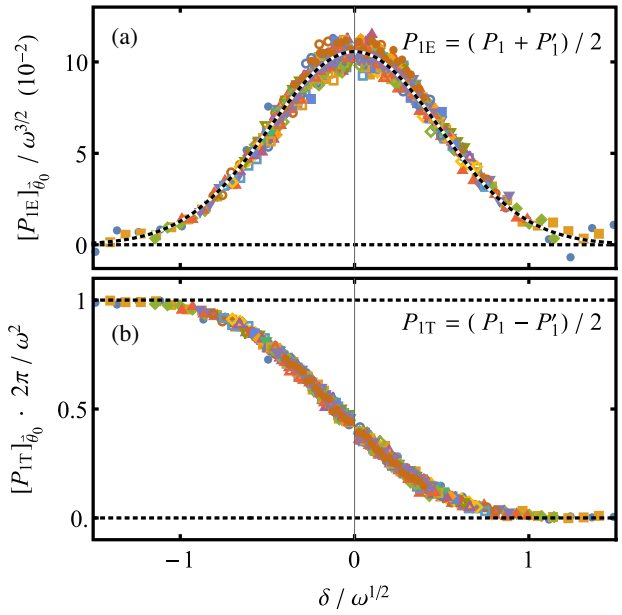

FIG. 3. The phase and time averaged excitation (top) and topological (bottom) scaling functions of the power averaged up to time $t\omega^{3/2} = 1.72$ ($t/t_u \approx 0.3$). As $p_{exc} \propto \mathcal{P}_{1E}$, the top panel is fit well by a Gaussian. The topological scaling function in the bottom panel decreases from one deep in the topological phase $\delta \ll -\omega^{1/2}$, to approximately one-half at the transition at $\delta = 0$ and to zero in the trivial phase. As δ is measured in units of $\omega^{1/2}$, the scaling function reproduces the step function in Eq. (9) in the limit $\omega \to 0$ at fixed δ. Parameters: $B_0 = 1$, ω_2/ω_1 is the golden ratio and 20 values of $\omega \in [0.0025, 0.1]$.

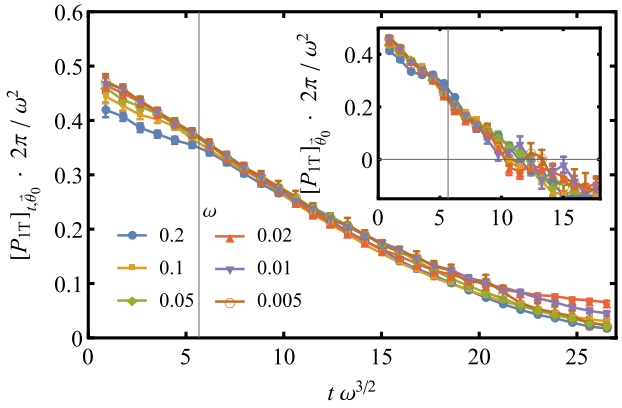

FIG. 4. The topological scaling function at the transition with (main) and without time averaging (inset). Both plots show that the scaling function approaches $1/2$ as $t\omega^{3/2} \to 0$, and zero as $t\omega^{3/2} \to \infty$. The vertical line is a proxy for t_u (definition in text). See the Supplemental Material [53] for the excitation scaling function at the transition.

quasiperiodic micromotion, and slightly modifies the value of the scaling function near $\delta = 0$. Scaling functions without time averaging are discussed in the Supplemental Material [53].

We now turn to the dependence of the scaling functions on t/t_u. Fig. 4 (inset) shows $\mathcal{P}_{1T} \sim [P_{1T}]_{\vec{\theta}_0}/P_Q$ at the transition, while the main figure shows the power with additional averaging over the time interval $[0, t]$. The gray vertical line is a proxy for t_u and identifies the mean time up to which $|\partial_t \vec{B}| < |\vec{B}|^2$. Both plots show that, as $t/t_u \to 0$, $\mathcal{P}_{1T}$ approaches the quantized value of

$$\mathcal{P}_{1T}(0;0) = \frac{1}{2}(C_g|_{\delta>0} + C_g|_{\delta<0}) = C_g|_{\delta=0} = \frac{1}{2}. \quad (15)$$

Next, for $0 < t/t_u \ll 1$, $\mathcal{P}_{1T}$ linearly decreases. This linear decrease follows from the constant excitation rate in Eq. (12) and the opposite sign of the pumping by the excited population. Finally, despite the negative turn at $t\omega^{3/2} \approx 10$ in the inset, we find that $\mathcal{P}_{1T}$ approaches zero for $t/t_u \gg 1$, consistent with the main figure.

Discussion—We have demonstrated that a simple quasiperiodically driven spin-$\frac{1}{2}$ exhibits universal scaling behaviors characteristic of extended classical or quantum *equilibrium* systems in the vicinity of continuous phase transitions [57,58]. Our results serve as a new example of the tantalizing correspondence emerging between equilibrium systems and systems subject to periodic or quasiperiodic driving [21–25,28–30,59–90].

The KZ scaling functions also provide the universal nonlinear response of a clean Dirac material in an electric field [91]. Fourier transforming the $\vec{\theta}$ coordinates maps the model in Eq. (2) on to the real-space model of a Hall insulator (the half-BHZ model) with an additional electric field (ω_1, ω_2). In this transformation, ω maps on to the magnitude of the electric field, the topological component of the power maps on to the Hall current, and the excitation component measures the population in the excited band due to dielectric breakdown when the insulator is initially at zero temperature.

Driven few-level systems can access other topological phase transitions in static systems using different driving protocols. Moreover, the KZ scaling theory can be extended to include the effects of dissipation [30], or counterdiabatic driving [25]. Both effects increase the unlock time t_u, and may simplify experimental access to the half-quantized response in solid-state and quantum optical platforms that host qubits [92–106].

We are grateful to E. Boyers, W. W. Ho, C. R. Laumann, D. Long, A. Polkovnikov, D. Sels, and A. Sushkov for useful discussions. This work was supported by NSF DMR-1752759 (A. C. and P. C.), and completed at the Aspen Center for Physics, which is supported by the NSF Grant No. PHY-1607611. A. C. and P. C. acknowledge support from the Sloan Foundation through the Sloan Research Fellowship. Work at Argonne was supported by the Department of Energy, Office of Science, Office of Basic Energy Sciences, Materials Science and Engineering Division.

*philip.jd.crowley@gmail.com

[1] H. E. Stanley, *Phase Transitions and Critical Phenomena* (Clarendon Press, Oxford, 1971).
[2] C. Domb and M. S. Green, *Phase Transitions and Critical Phenomena* (Academic Press, New York, 1972).
[3] J. J. Binney, N. J. Dowrick, A. J. Fisher, and M. E. Newman, *The Theory of Critical Phenomena: An Introduction to the Renormalization Group* (Oxford University Press, Oxford, 1992).
[4] N. D. Goldenfeld, *Lectures on Phase Transitions and the Renormalization Group* (Addison-Wesley, Reading, MA, 1992).
[5] P. M. Chaikin and T. Lubensky, *Principles of Condensed Matter Physics* (Cambridge University Press, Cambridge, England, 1995).
[6] S. Sachdev, *Quantum Phase Transitions* (Cambridge University Press, Cambridge, England, 2011).
[7] Y. K. Wang and F. Hioe, Phys. Rev. A **7**, 831 (1973).
[8] M. Henkel, H. Hinrichsen, S. Lübeck, and M. Pleimling, *Non-Equilibrium Phase Transitions* (Springer, New York, 2008), Vol. 1.
[9] J. Eisert and T. Prosen, arXiv:1012.5013.
[10] K. Baumann, C. Guerlin, F. Brennecke, and T. Esslinger, Nature (London) **464**, 1301 (2010).
[11] M. Karl, B. Nowak, and T. Gasenzer, Sci. Rep. **3**, 2394 (2013).
[12] L. M. Sieberer, S. D. Huber, E. Altman, and S. Diehl, Phys. Rev. Lett. **110**, 195301 (2013).
[13] C. Carr, R. Ritter, C. G. Wade, C. S. Adams, and K. J. Weatherill, Phys. Rev. Lett. **111**, 113901 (2013).

[14] U. C. Täuber, *Critical Dynamics: A Field Theory Approach to Equilibrium and Non-Equilibrium Scaling Behavior* (Cambridge University Press, Cambridge, England, 2014).
[15] M. Marcuzzi, E. Levi, S. Diehl, J. P. Garrahan, and I. Lesanovsky, Phys. Rev. Lett. **113**, 210401 (2014).
[16] J. Raftery, D. Sadri, S. Schmidt, H. E. Türeci, and A. A. Houck, Phys. Rev. X **4**, 031043 (2014).
[17] J. Klinder, H. Keßler, M. Wolke, L. Mathey, and A. Hemmerich, Proc. Natl. Acad. Sci. U.S.A. **112**, 3290 (2015).
[18] J. Marino and S. Diehl, Phys. Rev. Lett. **116**, 070407 (2016).
[19] U. C. Täuber, Annu. Rev. Condens. Matter Phys. **8**, 185 (2017).
[20] W. Casteels, R. Fazio, and C. Ciuti, Phys. Rev. A **95**, 012128 (2017).
[21] T. Ozawa and H. M. Price, Nat. Rev. Phys. **1**, 349 (2019).
[22] Y. Peng and G. Refael, Phys. Rev. B **97**, 134303 (2018).
[23] Y. Peng and G. Refael, Phys. Rev. B **98**, 220509 (2018).
[24] I. Martin, G. Refael, and B. Halperin, Phys. Rev. X **7**, 041008 (2017).
[25] P. J. D. Crowley, I. Martin, and A. Chandran, Phys. Rev. B **99**, 064306 (2019).
[26] J. H. Shirley, Phys. Rev. **138**, B979 (1965).
[27] H. Sambe, Phys. Rev. A **7**, 2203 (1973).
[28] T.-S. Ho, S.-I. Chu, and J. V. Tietz, Chem. Phys. Lett. **96**, 464 (1983).
[29] A. Verdeny, J. Puig, and F. Mintert, Z. Naturforsch. A **71**, 897 (2016).
[30] F. Nathan, I. Martin, and G. Refael, Phys. Rev. B **99**, 094311 (2019).
[31] B. A. Bernevig and T. L. Hughes, *Topological Insulators and Topological Superconductors* (Princeton University Press, Princeton, NJ, 2013).
[32] T. W. Kibble, J. Phys. A **9**, 1387 (1976).
[33] W. H. Zurek, Nature (London) **317**, 505 (1985).
[34] A. Polkovnikov, Phys. Rev. B **72**, 161201(R) (2005).
[35] W. H. Zurek, U. Dorner, and P. Zoller, Phys. Rev. Lett. **95**, 105701 (2005).
[36] J. Dziarmaga, Phys. Rev. Lett. **95**, 245701 (2005).
[37] S. Deng, G. Ortiz, and L. Viola, Europhys. Lett. **84**, 67008 (2009).
[38] J. Dziarmaga, Adv. Phys. **59**, 1063 (2010).
[39] G. Biroli, L. F. Cugliandolo, and A. Sicilia, Phys. Rev. E **81**, 050101(R) (2010).
[40] C. De Grandi, A. Polkovnikov, and A. W. Sandvik, Phys. Rev. B **84**, 224303 (2011).
[41] V. Gritsev and A. Polkovnikov, *Understanding Quantum Phase Transitions* (CRC Press, Boca Raton, 2010), pp. 59–90.
[42] A. Chandran, A. Erez, S. S. Gubser, and S. L. Sondhi, Phys. Rev. B **86**, 064304 (2012).
[43] M. Kolodrubetz, B. K. Clark, and D. A. Huse, Phys. Rev. Lett. **109**, 015701 (2012).
[44] A. D. Campo and W. H. Zurek, in *Symmetry and Fundamental Physics: Tom Kibble at 80* (World Scientific, Singapore, 2014), pp. 31–87.
[45] X.-L. Qi, Y.-S. Wu, and S.-C. Zhang, Phys. Rev. B **74**, 085308 (2006).
[46] B. A. Bernevig, T. L. Hughes, and S.-C. Zhang, Science **314**, 1757 (2006).
[47] P. Weinberg, M. Bukov, L. D'Alessio, A. Polkovnikov, S. Vajna, and M. Kolodrubetz, Phys. Rep. **688**, 1 (2017).
[48] G. Rigolin, G. Ortiz, and V. H. Ponce, Phys. Rev. A **78**, 052508 (2008).
[49] C. De Grandi and A. Polkovnikov, in *Quantum Quenching, Annealing and Computation* (Springer, New York, 2010), pp. 75–114.
[50] C. Zener, Proc. R. Soc. A **137**, 696 (1932).
[51] L. Landau, Phys. Z. Sowjetunion **11**, 26 (1937) [JETP **7**, 1 (1937)].
[52] L. Landau, Phys. Z. Sowjetunion **11**, 545 (1937) [JETP **7**, 627 (1937)].
[53] See Supplemental Material at http://link.aps.org/supplemental/10.1103/PhysRevLett.125.100601 where we obtain the same scaling functions for a different microscopic model with a Dirac transition, demonstrating universality; and discuss their properties in the absence of the time averaging used in the main text, which includes Refs. [31,45,54–56].
[54] M. Z. Hasan and C. L. Kane, Rev. Mod. Phys. **82**, 3045 (2010).
[55] A. Bansil, H. Lin, and T. Das, Rev. Mod. Phys. **88**, 021004 (2016).
[56] D. R. Hofstadter, Phys. Rev. B **14**, 2239 (1976).
[57] J. Cardy, *Scaling and Renormalization in Statistical Physics* (Cambridge University Press, Cambridge, England, 1996), Vol. 5.
[58] S. Sachdev, Phys. World **12**, 33 (1999).
[59] J. Luck, H. Orland, and U. Smilansky, J. Stat. Phys. **53**, 551 (1988).
[60] H. Jauslin and J. Lebowitz, Chaos **1**, 114 (1991).
[61] P. Blekher, H. Jauslin, and J. Lebowitz, J. Stat. Phys. **68**, 271 (1992).
[62] H. Jauslin and J. Lebowitz, in *Mathematical Physics X* (Springer, New York, 1992), pp. 313–316.
[63] T. Kitagawa, T. Oka, A. Brataas, L. Fu, and E. Demler, Phys. Rev. B **84**, 235108 (2011).
[64] N. H. Lindner, G. Refael, and V. Galitski, Nat. Phys. **7**, 490 (2011).
[65] L. Jiang, T. Kitagawa, J. Alicea, A. R. Akhmerov, D. Pekker, G. Refael, J. I. Cirac, E. Demler, M. D. Lukin, and P. Zoller, Phys. Rev. Lett. **106**, 220402 (2011).
[66] J. Cayssol, B. Dóra, F. Simon, and R. Moessner, Phys. Status Solidi RRL **7**, 101 (2013).
[67] Y. T. Katan and D. Podolsky, Phys. Rev. Lett. **110**, 016802 (2013).
[68] M. S. Rudner, N. H. Lindner, E. Berg, and M. Levin, Phys. Rev. X **3**, 031005 (2013).
[69] T. Iadecola, D. Campbell, C. Chamon, C.-Y. Hou, R. Jackiw, S.-Y. Pi, and S. V. Kusminskiy, Phys. Rev. Lett. **110**, 176603 (2013).
[70] P. Delplace, Á. Gómez-León, and G. Platero, Phys. Rev. B **88**, 245422 (2013).
[71] A. Kundu, H. A. Fertig, and B. Seradjeh, Phys. Rev. Lett. **113**, 236803 (2014).

[72] A. G. Grushin, Á. Gómez-León, and T. Neupert, Phys. Rev. Lett. **112**, 156801 (2014).
[73] M. Lababidi, I. I. Satija, and E. Zhao, Phys. Rev. Lett. **112**, 026805 (2014).
[74] A. Chandran and S. L. Sondhi, Phys. Rev. B **93**, 174305 (2016).
[75] V. Khemani, A. Lazarides, R. Moessner, and S. L. Sondhi, Phys. Rev. Lett. **116**, 250401 (2016).
[76] C. W. von Keyserlingk and S. L. Sondhi, Phys. Rev. B **93**, 245145 (2016).
[77] C. W. von Keyserlingk and S. L. Sondhi, Phys. Rev. B **93**, 245146 (2016).
[78] R. Roy and F. Harper, Phys. Rev. B **94**, 125105 (2016).
[79] D. V. Else and C. Nayak, Phys. Rev. B **93**, 201103 (2016).
[80] F. Nathan, M. S. Rudner, N. H. Lindner, E. Berg, and G. Refael, Phys. Rev. Lett. **119**, 186801 (2017).
[81] R. Roy and F. Harper, Phys. Rev. B **96**, 155118 (2017).
[82] R. Moessner and S. Sondhi, Nat. Phys. **13**, 424 (2017).
[83] Y. Baum and G. Refael, Phys. Rev. Lett. **120**, 106402 (2018).
[84] I. Mondragon-Shem, I. Martin, A. Alexandradinata, and M. Cheng, arXiv:1811.10632.
[85] M. H. Kolodrubetz, F. Nathan, S. Gazit, T. Morimoto, and J. E. Moore, Phys. Rev. Lett. **120**, 150601 (2018).
[86] P. T. Dumitrescu, R. Vasseur, and A. C. Potter, Phys. Rev. Lett. **120**, 070602 (2018).
[87] Y. Peng and G. Refael, Phys. Rev. Lett. **123**, 016806 (2019).
[88] B. Bauer, T. Pereg-Barnea, T. Karzig, M.-T. Rieder, G. Refael, E. Berg, and Y. Oreg, Phys. Rev. B **100**, 041102(R) (2019).
[89] H. Hu, B. Huang, E. Zhao, and W. V. Liu, Phys. Rev. Lett. **124**, 057001 (2020).
[90] T. Oka and S. Kitamura, Annu. Rev. Condens. Matter Phys. **10**, 387 (2019).
[91] A. G. Green and S. L. Sondhi, Phys. Rev. Lett. **95**, 267001 (2005).
[92] F. Jelezko, T. Gaebel, I. Popa, M. Domhan, A. Gruber, and J. Wrachtrup, Phys. Rev. Lett. **93**, 130501 (2004).
[93] I. Buluta, S. Ashhab, and F. Nori, Rep. Prog. Phys. **74**, 104401 (2011).
[94] J. Clarke and F. K. Wilhelm, Nature (London) **453**, 1031 (2008).
[95] V. Dobrovitski, G. Fuchs, A. Falk, C. Santori, and D. Awschalom, Annu. Rev. Condens. Matter Phys. **4**, 23 (2013).
[96] C. Kloeffel and D. Loss, Annu. Rev. Condens. Matter Phys. **4**, 51 (2013).
[97] H. Häffner, C. F. Roos, and R. Blatt, Phys. Rep. **469**, 155 (2008).
[98] M. H. Devoret, A. Wallraff, and J. M. Martinis, arXiv: cond-mat/0411174.
[99] C. Langer, R. Ozeri, J. D. Jost, J. Chiaverini, B. DeMarco, A. Ben-Kish, R. Blakestad, J. Britton, D. Hume, W. M. Itano, D. Leibfried, R. Reichle, T. Rosenband, T. Schaetz, P. O. Schmidt, and D. J. Wineland, Phys. Rev. Lett. **95**, 060502 (2005).
[100] J. Taylor, H.-A. Engel, W. Dür, A. Yacoby, C. Marcus, P. Zoller, and M. Lukin, Nat. Phys. **1**, 177 (2005).
[101] B. Trauzettel, D. V. Bulaev, D. Loss, and G. Burkard, Nat. Phys. **3**, 192 (2007).
[102] A. Gali, Phys. Rev. B **79**, 235210 (2009).
[103] R. Blatt and C. F. Roos, Nat. Phys. **8**, 277 (2012).
[104] T. P. Harty, D. T. C. Allcock, C. J. Ballance, L. Guidoni, H. A. Janacek, N. M. Linke, D. N. Stacey, and D. M. Lucas, Phys. Rev. Lett. **113**, 220501 (2014).
[105] G. Wendin, Rep. Prog. Phys. **80**, 106001 (2017).
[106] Y. Wang, M. Um, J. Zhang, S. An, M. Lyu, J.-N. Zhang, L.-M. Duan, D. Yum, and K. Kim, Nat. Photonics **11**, 646 (2017).